



Precise Direction Detector: Indoor Localization System Based on Commodity Wi-Fi

Xiaolong Yang^(✉), Xin Yu, Jiacheng Wang, Qing Jiang, and Mu Zhou

Chongqing Key Lab of Mobile Communications Technology,
Chongqing University of Posts and Telecommunications, Chongqing 400065, China
yangxiaolong@cqupt.edu.cn

Abstract. This paper aims to present a novel algorithm for indoor localization by employing the channel state information (CSI) which is collected by Wi-Fi chips that are on common Wi-Fi device to estimate the angle of arrival (AoA) of multipath components accurately. In a complex indoor environment, the proposed direct path identification algorithm can be used to identify the line of sight (LOS) and non-line of sight (NLOS) scenario with the averaged detection rates of 0.814 and 0.920, respectively. Finally, by using the widely-known least squares localization algorithm to locate the target. Extensive experimental results have demonstrated that our system can achieve the median localization error of 0.7 m and be robust to the environment variations.

Keywords: Wi-Fi · Indoor localization · Channel state information (CSI) · Angle of arrival (AoA)

1 Introduction

With the rapid growth of Wi-Fi infrastructure and devices, a booming increase of applications based on indoor localization has been witnessed [1], such as shopping navigation [2] and augmented reality [3]. The mainstream of Wi-Fi localization systems is based on the received signal strength (RSS), location fingerprinting, time of flight (ToF), and angle of arrival (AoA). The RSS-based system measures RSS from multiple APs to build the propagation models, and then uses the triangulation approach [4] to locate the target. Another popular system is based on location fingerprinting, which collects the fingerprints, such as the RSS, to build a relationship between the fingerprints and physical locations [5]. Benefiting from the multiple input multiple output (MIMO), the AoA-based system has been carefully studied. The basic idea is to use the antenna array to calculate the AoA of multipath signal at the wireless access point (AP). Besides, there

Supported by the Science and Technology Research Program of Chongqing Municipal Education Commission (Grant No. KJQN201800625).

are some other existing indoor localization systems based on radio frequency identification (RFID) [6] and ultra-wideband (UWB) [7]. Summary Cognitive radio has attracted considerable attention because of its ability to make full use of the available spectrum resources for wireless terrestrial communication networks [8–10].

The most accurate systems, like the ArrayTrack [1] and Ubicarse [11], can reach an accuracy of 30–50 cm in indoor environment. However, these systems cannot meet the requirements of cost efficiency and universality, which make them hard to apply. The ArrayTrack and LTEye [12] work on AoA estimation which are accurate and universal, but they both need to modify the hardware. The ArrayTrack requires the AP to be equipped with 6 to 8 antennas, which contradict the common AP with three or less antennas. SpotFi [12] overcomes the constraints on number of antennas, but still cannot solve the problem of coherent signal and need the help of received signal strength indicator (RSSI) to complete localization. The LTEye uses the motorized rotating antenna which is more difficult to be applied. Other localization systems, such as the Ubicarse and Wi-Fi/MEMS system [13], can also be cost-efficient and accurate by combining the data from different sensors, but they require the target to be equipped with accelerometer and gyroscope, which are hardly found in many types of terminals.

2 System Description

2.1 Super-Precision Estimation Model

It is known that the signals experience the attenuation and time delay during the propagation, and there are generally 6–8 significant propagation paths in dense indoor multipath environment [1]. So we describe the channel frequency response (CFR) as

$$h(f) = \sum_{l=0}^k \gamma_l e^{-j2\pi f \tau_l}, \quad (1)$$

where γ_l is the attenuation, τ_l is the time delay and f denotes the frequency of the transmitted signal. The CSI can be recognized as a sample edition of the CFR.

For the k th propagation path, τ_k is the distance from the AP to receiver, d is the antenna spacing, and θ_k is the signal incident angle. Thus, the received signals at the m th antenna travels an additional distance $d(m-1)\sin\theta$, which results in a phase shift $-2\pi \times (m-1) \times d \times \sin(\theta_k) \times f_0/c$. Then the phase shift related to AoA on the k th propagation path, at the m th antenna can be described as

$$\Phi(\theta_k, \tau_k) = e^{-j2\pi f \times d \times (m-1) \times \sin(\theta_k)/c}, \quad (2)$$

where c is the speed of light. The vector of received signals on the k th path can be written as

$$\mathbf{a}(\theta_k, \tau_k) = [1 \ \Phi(\theta_k, \tau_k) \cdots \Phi(\theta_k, \tau_k)^{m-1}]^T. \quad (3)$$

By assuming that there are L propagation paths, we define the steering matrix as

$$\mathbf{A} = [\mathbf{a}(\theta_1, \tau_1), \dots, \mathbf{a}(\theta_L, \tau_L)]. \quad (4)$$

Thereby, the received signal is constructed with the superposition of multi-path signal, which can be expressed as

$$\mathbf{x} = \sum_{i=1}^L (\mathbf{a}(\theta_i, \tau_i) \gamma_i + n_i) = \mathbf{A} \boldsymbol{\Gamma} + \mathbf{N}, \quad (5)$$

where $\boldsymbol{\Gamma}$ denotes the vector of attenuations on the L paths and \mathbf{N} is the noise. Then, we build the measurement \mathbf{X} through received signal vectors for N subcarriers

$$\mathbf{X} = [\mathbf{x}_1 \cdots \mathbf{x}_N] = \mathbf{A} [\boldsymbol{\Gamma}_1 \cdots \boldsymbol{\Gamma}_N], \quad (6)$$

where $[\mathbf{x}_1 \cdots \mathbf{x}_N]$ denotes the vectors obtained from all subcarriers and $[\boldsymbol{\Gamma}_1 \cdots \boldsymbol{\Gamma}_N]$ are the corresponding complex attenuation. The impact of channel on signals is entirely recorded in CSI which is presented by Wi-Fi card. So, for a system equipped with Intel 5300 and 3 antennas, the CSI matrix can be expressed as

$$\text{CSI} = \begin{bmatrix} \overbrace{c_{1,1} \cdots c_{1,30}}^{\text{antenna1}} & \overbrace{c_{2,1} \cdots c_{2,30}}^{\text{antenna2}} & \overbrace{c_{3,1} \cdots c_{3,30}}^{\text{antenna3}} \end{bmatrix} = \begin{bmatrix} c_{1,1} & c_{1,2} & \cdots & c_{1,30} \\ c_{2,1} \cdots c_{2,3} & \cdots & c_{2,30} \\ c_{3,1} \cdots c_{3,4} & \cdots & c_{3,30} \end{bmatrix}. \quad (7)$$

The goal of our system is to use \mathbf{X} to estimate \mathbf{A} . The AoA can be easily estimated when \mathbf{A} has been obtained. The multiple signal classification (MUSIC) algorithm works well for the relations between \mathbf{A} and \mathbf{X} , because the eigenvectors of $\mathbf{X}\mathbf{X}^H$ corresponding to the eigenvalue 0 are orthogonal to the steering vectors in \mathbf{A} . \mathbf{X}^H is the conjugate transpose of \mathbf{X} . Thus, we calculate the eigenvectors of $\mathbf{X}\mathbf{X}^H$ corresponding to the eigenvalue 0, construct the steering vectors which are orthogonal to the eigenvectors, and extract the AoA from the steering vectors. The covariance matrix \mathbf{R}_x with respect to the received signal is expressed as

$$\begin{aligned} \mathbf{R}_x &= E[\mathbf{X}\mathbf{X}^H] \\ &= \mathbf{A}E[\mathbf{S}\mathbf{S}^H]\mathbf{A}^H + E[\mathbf{N}\mathbf{N}^H], \\ &= \mathbf{A}\mathbf{R}_s\mathbf{A}^H + \sigma^2\mathbf{I} \end{aligned} \quad (8)$$

where \mathbf{R}_s is the covariance matrix of signal vectors. As we know, the smallest $90 - L$ eigenvalues are corresponding to the noise subspace, while the other L eigenvalues are corresponding to the signal subspace. Based on this, we employ the spatial spectrum function in (9) to estimate the steering vectors $\mathbf{a}(\theta, \tau)$ when the denominator is close to 0. Then, the angle corresponding to sharp peak is selected as the incident angle of the AoA.

$$P(\theta, \tau)_{MUSIC} = \frac{1}{\mathbf{a}(\theta, \tau)^H \mathbf{E}_N \mathbf{E}_N^H \mathbf{a}(\theta, \tau)}. \quad (9)$$

2.2 CSI Matrix Smoothing and Direct Path Identification

In indoor environment, the received signals are likely to be coherent, which is not beneficial for the angle estimation. To address this issue, our system performs spatial smoothing on \mathbf{R}_x . The covariance matrices are constructed by increasing the serial number of subcarriers from 1 to $E_2 = 30 - N_2 + 1$ and the serial number of antennas from 1 to $E_1 = 3 - N_1 + 1$. In our system, $N_2 = 15$ and $N_1 = 2$. Then, the total number of sub-arrays and the elements in each sub-array equals to $E_1 \times E_2$ and $N_1 \times N_2$. In this case, the covariance matrix of CSI can be modified into

$$\mathbf{R}_{smoothed} = \frac{1}{\mathbf{E}_1 \times \mathbf{E}_2} \sum_{i=1}^{\mathbf{E}_1} \sum_{j=1}^{\mathbf{E}_2} \mathbf{R}_{i,j}. \quad (10)$$

The $\mathbf{R}_{i,j}$ is the sub-covariance matrix of \mathbf{R}_x , which can be written as

$$\mathbf{R}_{i,j} = \begin{bmatrix} x_{i,j} \times x_{i,j} & \cdots \cdots & x_{i,j} \times x_{i+1,j+15-1} \\ \vdots & \vdots \vdots & \vdots \\ x_{i,j+15-1} \times x_{i,j} & \cdots \cdots & x_{i,j+15-1} \times x_{i+1,j+15-1} \\ x_{i+1,j} \times x_{i,j} & \cdots \cdots & x_{i+1,j} \times x_{i+1,j+15-1} \\ \vdots & \vdots \vdots & \vdots \\ x_{i+1,j+15-1} \times x_{i,j} & \cdots \cdots & x_{i+1,j+15-1} \times x_{i+1,j+15-1} \end{bmatrix}, \quad (11)$$

where $x_{i,j} \times x_{i,j}$ is the first element of the sub-covariance matrix.

In the direct path identification section, we use least squares method to get better fitting effect. First, we perform the affinity propagation clustering on the peak points from the result of MUSIC. Second, to detect the outliers, we calculate the density of each point by

$$\rho(\mathbf{x}, k) = \left(\frac{\sum_{\mathbf{y} \in N(\mathbf{x}, k)} d(\mathbf{x}, \mathbf{y})}{|N(\mathbf{x}, k)|} \right)^{-1}, \quad (12)$$

where $N(\mathbf{x}, k)$ is the set of k nearest neighbors of \mathbf{x} , $|N(\mathbf{x}, k)|$ denotes the size of set $N(\mathbf{x}, k)$, and \mathbf{y} refers to the nearest point. We divide (12) by the averaged density of its k nearest neighbors to obtain the average relative density.

$$\bar{\rho}(\mathbf{x}, k) = \frac{\rho(\mathbf{x}, k)}{\left(\sum_{\mathbf{y} \in N(\mathbf{x}, k)} d(\mathbf{y}, k) / |N(\mathbf{x}, k)| \right)}. \quad (13)$$

Third, an outlier score is distributed to each point and the points with significantly high scores need to be deleted. The algorithm used for outlier deletion is described in Algorithm 1.

Finally, we select the path with the highest score as the direct one to locate the target by

$$score_i = \exp(\alpha_n N_i - \alpha_\theta \sigma_{\theta_i} - \alpha_\tau \sigma_{\tau_i} - \alpha_{m\tau} \bar{\tau}_i). \quad (14)$$

In the i th cluster, where σ_{θ_i} and σ_{τ_i} stand for the variance of AoA and ToA of the points, N_i denotes the number of points, and $\bar{\tau}_i$ is the average ToF of the points. Besides, α_n , α_θ , α_τ , and $\alpha_{m\tau}$ express the weights.

Algorithm 1. Outlier Deletion

Input: Raw data from one cluster
Output: Modified data without outliers

```

1 if the number of point in cluster > 5 then
2   for all  $x$  do
3     | determine  $N(x, k)$ ; calculate  $\rho(x, k)$ ;
4   end
5   for all  $x$  do
6     | distribute an outlier score to each point, outlier score=average relative
7     |  $\rho(x, k)$ ;
8   end
9   if the number of point in cluster < 10 then
10    | delete the point with the highest outlier score from  $x$ ;
11  else
12    | delete (the number of point*0.1) outliers
13  end
14 end

```

3 Experiments and Evaluation

As shown in Fig. 1, 27 test points are uniformly calibrated with every two adjacent points spacing 0.6 m in each column and the distance interval between the neighboring columns of test points is about 3 m.

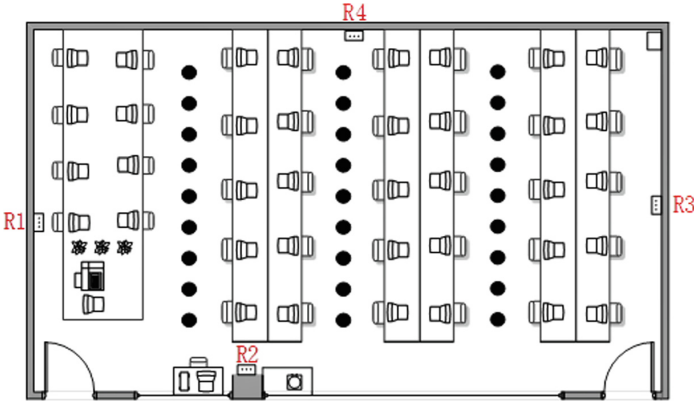


Fig. 1. Testbed of indoor environment

So as to verify the ability of system to identify LOS and NLOS, we place 4 APs in which two of them are blocked with the metal plates to create NLOS scenario during the tests and analyze its detection rate. In LOS and NLOS

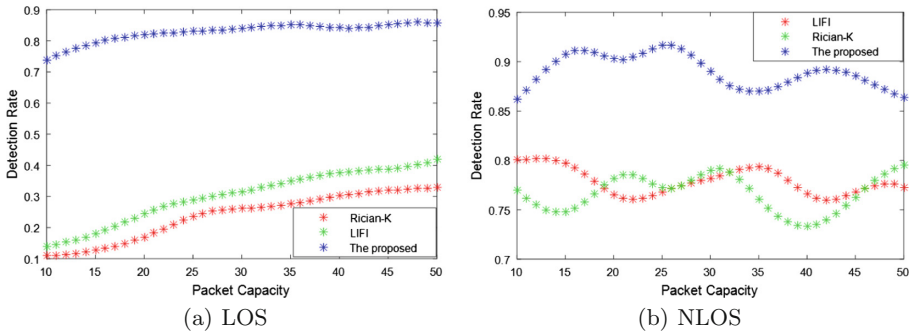
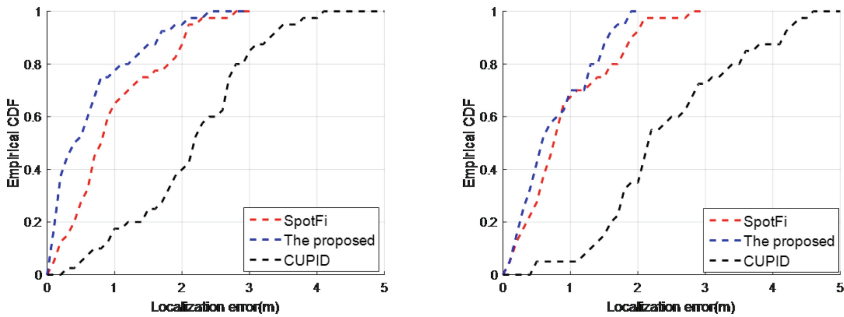


Fig. 2. Detection rate in LOS and NLOS scenarios

scenarios, compared with other two typical systems, namely the LIFI [14] and Rician-K, we can see from Fig. 2(a) and (b) that the proposed system can at least achieves the detection rates above 0.7 and 0.85, respectively. While the two typical systems only can at most achieve the detection rates of 0.42 and 0.8. Besides, the proposed system achieves the higher averaged detection rates of 0.814 and 0.920 in this two scenarios, respectively.

For comparison, the schemes proposed in SpotFi and CUPID [15] are also used to process the same data. From Fig. 3(a) we can see that the proposed system achieves higher positioning accuracy with the median error of 0.502 m, while the SpotFi and CUPID are only with the median errors of 0.652 m and 2.12 m, respectively.



(a) Localization errors in indoor environment (b) Localization errors for the off-the-shelf smartphone

Fig. 3. Localization errors in indoor environment

To verify the practicability of our system, we select the off-the-shelf Samsung i9500 smartphone as the target for the testing. The tester holding the smartphone walks around with random directions in detected area. Each receiver collects 100 packets per second and 20 of them are used to locate the target. As we can see in

Fig. 3(b), when the experimental condition become complex, the performance of CUPID degrade significantly which can only reach a median accuracy of 2.57 m. Obviously, the proposed plan is more robust than CUPID and SpotFi which can achieve an impressive median accuracy of 0.7 m, while SpotFi can only reach 0.743 m.

4 Conclusions

In this paper, the proposed system is proved to be able to estimate the AoA and ToF of the signal accurately based on the existing Wi-Fi device without any extra hardware. At the same time, the smoothing algorithm can resist the coherent signal effectively. Furthermore, our system is capable of picking out the APs operating in LOS scenario with high detection rate and extracting the information of direct path to locate the target. The extensive experiments conducted in the indoor environments demonstrate its robustness and practicability. In the future, we will continue to investigate the approach of self-adaptive threshold setting to improve the detection rate of direct path in NLOS scenario.

References

1. Xiong, J., Jamieson, K.: ArrayTrack: a fine-grained indoor location system. In: USENIX Conference on Networked Systems Design and Implementation, Lombard, IL, USA, pp. 71–84 (2013)
2. Shu, Y., et al.: Last-mile navigation using smartphones. In: International Conference on Mobile Computing and Networking ACM, Paris, France, pp. 512–524 (2015)
3. Wang, H., Bao, X., Roy Choudhury, R., Nelakuditi, S.: Visually fingerprinting humans without face recognition. In: Proceedings of the ACM MobiSys, Paris, France, pp. 345–358 (2015)
4. Tian, Z., et al.: Fingerprint indoor positioning algorithm based on affinity propagation clustering. *EURASIP J. Wirel. Commun. Netw.* 1–8 (2013)
5. Youssef, M.: The Horus WLAN location determination system. In: International Conference on Mobile Systems, Applications, and Services, Seattle, Washington, USA, pp. 205–218 (2005)
6. Wang, J., Katabi, D.: Dude, where’s my card? RFID positioning that works with multipath and non-line of sight. In: Proceedings of the ACM SIGCOMM 2013 Conference on SIGCOMM, Hong Kong, China, pp. 51–62 (2013)
7. Wang, J., Vasisht, D., Katabi, D.: RF-IDraw: virtual touch screen in the air using RF signals. In: ACM SIGCOMM Computer Communication Review, Maui, Hawaii, pp. 1–4 (2014)
8. Jia, M., Gu, X., Guo, Q., Xiang, W., Zhang, N.: Broadband hybrid satellite-terrestrial communication systems based on cognitive radio toward 5G. *IEEE Wirel. Commun.* **23**, 96–106 (2016)
9. Jia, M., Liu, X., Gu, X., Guo, Q.: Joint cooperative spectrum sensing and channel selection optimization for satellite communication systems based on cognitive radio. *Int. J. Satell. Commun. Netw.* **35**, 139–150 (2017)

10. Jia, M., Liu, X., Yin, Z., Guo, Q., Gu, X.: Joint cooperative spectrum sensing and spectrum opportunity for satellite cluster communication networks. *Ad Hoc Netw.* **58**, 231–238 (2016)
11. Kumar, S., Gil, S., Katabi, D., Rus, D.: Accurate indoor localization with zero start-up cost. In: *International Conference on Mobile Computing and Networking*, Maui, Hawaii, USA, pp. 483–494 (2014)
12. Kotaru, M., Joshi, K., Bharadia, D., et al.: SpotFi: decimeter level localization using WiFi. In: *ACM Conference on Special Interest Group on Data Communication*, London, United Kingdom, pp. 269–282 (2015)
13. Tian, Z., et al.: Smartphone-based indoor integrated WiFi/MEMS positioning algorithm in a multi-floor environment. *Micromachines* **6**(3), 347–363 (2015)
14. Zhou, Z., et al.: LiFi: line-of-sight identification with WiFi. In: *INFOCOM IEEE*, Toronto Canada (2014)
15. Sen, S., et al.: Avoiding multipath to revive inbuilding WiFi localization. In: *Proceeding of the, International Conference on Mobile Systems, Applications, and Services ACM*, pp. 249–262 (2013)